Demonstration of Autonomous Orbit Determination Around Small Bodies

S. Bhaskaran and J. E. Riedel
Jet Propulsion Laboratory
California Institute of Technology
Pasadena, California

1 Introduction

The navigation of spacecraft orbiting small objects such as asteroids or comets presents special problems not seen in planetary orbiting missions. In particular, the dynamic environment the spacecraft is operating in may be changing quickly due to perturbations from the gravity field and solar radiation pressure. Maneuvers are then needed fairly often to maintain the orbit. Navigating the spacecraft using conventional ground-based methods may be very costly in terms of staffing requirements to keep personnel around the clock to perform orbit determination and maneuver analysis functions. It, may also prove to be impractical to navigate from the ground due to frequent maneuvers and long round-trip light times. For these reasons, the feasibility of performing some or all of the navigation functions onboard the spacecraft is being looked into. This study addresses the problem of onboard orbit determination of a spacecraft around a small object. It is assumed that an important first step to any autonomous scheme for orbiting small objects - building a model of the object itself - has been done and is available. An algorithm has been developed which uses this precomputed shape model of the object and images taken with a wide field-of-view (FOV) camera to autonomously determine the state of the spacecraft. The method is demonstrated with the use of a simulation.

2 Equipment

The sole instrument used to obtain data is a camera with a wide FOV (around 50 to 60 degrees) and a fairly short focal length (50 to 100 mm). The exact specifications of the camera will depend on the particular mission; for this simulation, an 800x800 pixel array camera with a 60 deg. FOV and 50 mm focal length was chosen. The wide FOV is necessary to keep the entire object within the camera frame even at fairly close distances. in addition, these specifications ensure that epected errors in camera pointing obtained independently of the imaging camera will be at the sub-pixel level and can be ignored for the simulation.

3 Procedure

A brief outline of the procedure used by the algorithm will now be described. As mentioned earlier, it is assumed that a precomputed model of the object is available to the algorithm. With this information and a nominal orbit, predicted scenes seen by the camera at the predetermined exposure times arc computed. The actual picture taken by the camera is then compared with the predicted, and this information is then used to adjust the nominal orbit.

The comparison is done by first determining the edges of the predicted picture on all four sides of the object. This results in plots of the limb location as a function of the line number (for vertical edges) or pixel number (for horizontal edges). The same edge detection is performed on the observed picture taken by the camera, The predicted limbs are then broken up into segments with lengths of about 100 to 120 pixels. Depending on the size of the object in the frame, this results in 1 to 3 limb segments for a given side. The pixel and line coordinates of the center point of each of these limb sections (hereafter called the "anchor" point) Will be needed later. The segments are then correlated with the corresponding observed limbs to find where each segment best matches the observation. The average shift in pixel and line needed to best fit the predicted limb section to the actual limb becomes one set of observables. ~'bus, each predicted limb section which correlates with an actual limb contributes a set of observable, which will then be used in a least squares fit.

Since the predicted limbs are found using a known shape model, the coordinates of the anchor points, along with the nominal orbit information, can be used to determine the nominal vectors from the camera to the anchor points. This enables the computation of numerical partial derivatives of the])ixd/line shift with respect to the nominal state (position in x, y, and z) to form the information matrix. '1'bus, a standard least squares fit problem is formed, with the residuals being the shift vectors mentioned above, and the estimated state being the instantaneous position at the time of the picture. 'J'befit also produces formal statistics of the estimate which can be used to determine the effectiveness of the algorithm.

4 Simulation and Results

In order to test tile algorithm, simulations of orbits around a realistic looking, irregularly shaped asteroid were performed. The asteroid's dimensions were roughly 40x20x20 km. Two orbits were tried, one at a radius of 50 km, and one at 100 km. Both orbits were in planes which were nearly perpendicular to the sunline, so the phase angles varied from a minimum of 40 deg. to a maximum of 130 deg.

The procedure for the simulation was as follows. First, a nominal orbit was generated, and simulated pictures of the asteroid were taken using the geometry from the nominal orbit. Then, the initial conditions were perturbed, and a new orbit representing the "truth" was generated with the perturbed state. simulated pictures taken with geometry from the "true" orbit are used to the get the observed limbs. The algorithm is then called to compute corrections to the nominal state at each time step where a picture was taken, as described above. Finally, the estimated position is compared to the known "truth" to see if the errors are within the formal uncertainties computed by the filter.

A p]ot of the computed position errors at ten picture locations for the 100 km orbit around an asteroid is shown in Figure 1. In addition, the 1-sigma standard deviation of the fit is also plotted. It can be seen that the algorithm successfully determined the position of the spacecraft to within 1-sigma for all cases except the y position in the tenth picture, which had an estimate slightly less than 2-sigma. Similiar results were seen in the simulation at the 50 km orbit.

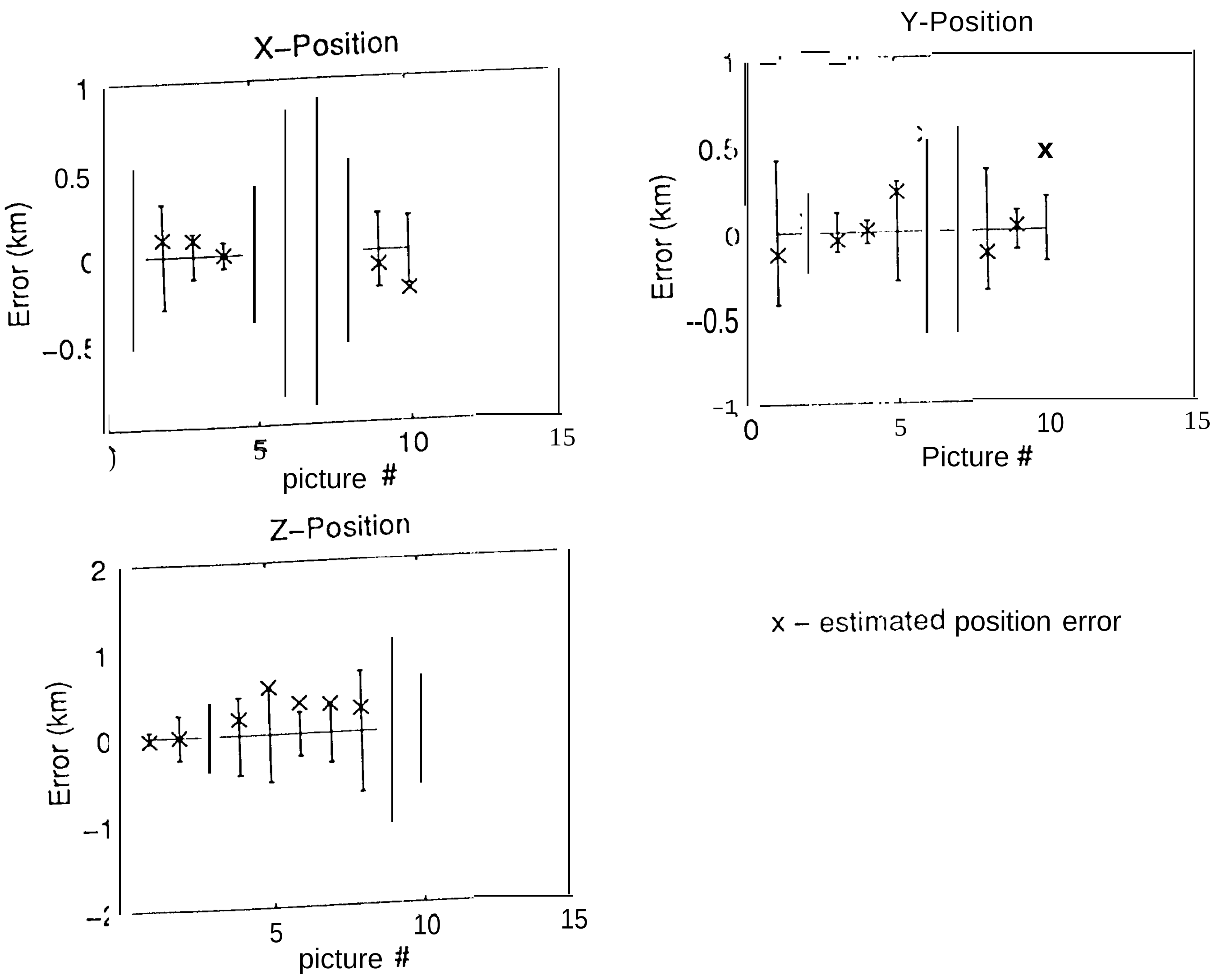

Figure 1: Position Errors and 1-sigma Uncertainties